High Spatial Resolution Coronary Magnetic Resonance Angiography: A Single Center Experience

Reza Hajhosseiny[1]; Aurélien Bustin[1]; Imran Rashid[1]; Gastao Cruz[1]; Karl P. Kunze[1,2]; Radhouene Neji[1,2]; Ronak Rajani[3]; Claudia Prieto[1]; René M. Botnar[1]

[1]School of Biomedical Engineering and Imaging Sciences, King's College London, London, United Kingdom
[2]MR Research Collaborations, Siemens Healthcare Limited, Frimley, United Kingdom
[3]School of Cardiovascular Medicine and Sciences, King's College London, London, United Kingdom

Abstract

Coronary magnetic resonance angiography (CMRA) could potentially offer a safe, non-invasive alternative for the anatomical assessment of coronary artery disease (CAD), which is free of ionizing radiation and iodinated contrast agents. However, image acquisition with conventional free-breathing CMRA frameworks is limited by long and unpredictable scan times, whilst image degradation due to respiratory motion remains a challenge. Here we outline a CMRA framework, that aims to overcome some of these challenges by incorporating a highly undersampled Cartesian acquisition with a two-dimensional (2D) image navigator to enable 100% respiratory scan efficiency, 2D translational motion correction, and three-dimensional (3D) non-rigid motion estimation, which is then fully reconstructed using a 3D patch-based low-rank regularization framework (PROST)[1]. We recently validated this framework against coronary computed tomography angiography (CCTA) in a single-center trial of 50 patients with suspected CAD. Diagnostic image quality was obtained in 95% of all coronary segments. The sensitivity, specificity, and negative predictive value were as follows: per-patient, 100%, 74%, and 100%; per-vessel, 81%, 88%, and 97%; and per-segment, 76%, 95%, and 99%, respectively. These findings emphasize the growing potential of this CMRA framework as a viable alternative to CCTA and invasive X-ray angiography for the anatomical assessment of CAD.

Introduction

Cardiovascular disease is the leading cause of mortality worldwide [1]. Among all causes of cardiovascular disease, atherosclerotic coronary artery disease (CAD) accounts for approximately half of all cases [1]. The early detection and long-term monitoring of CAD enable targeted risk stratification and prophylactic treatment of patients most at risk of progressing toward acute coronary syndromes. Invasive X-ray coronary angiography and non-invasive coronary computed tomography angiography (CCTA) are the gold standard imaging modalities for the assessment of CAD [2–7]. Despite being highly diagnostic, X-ray coronary angiography is limited by invasive complications (e.g., death, stroke, myocardial and vascular injury, pain, and bleeding), whilst both X-ray coronary angiography and CCTA are limited by the risks from ionizing radiation and contrast-mediated nephropathy. There is therefore a clear need for an alternative imaging modality for the early detection and long-term monitoring of CAD, which is free of the risks associated with X-ray coronary angiography and CCTA.

Coronary magnetic resonance angiography

Cardiovascular magnetic resonance (CMR) could be a safe, non-invasive alternative for the imaging of coronary artery stenosis without ionizing radiation or iodinated contrast

[1]*Work in progress. The application is currently under development and is not for sale in the U.S. and in other countries. Its future availability cannot be ensured.*

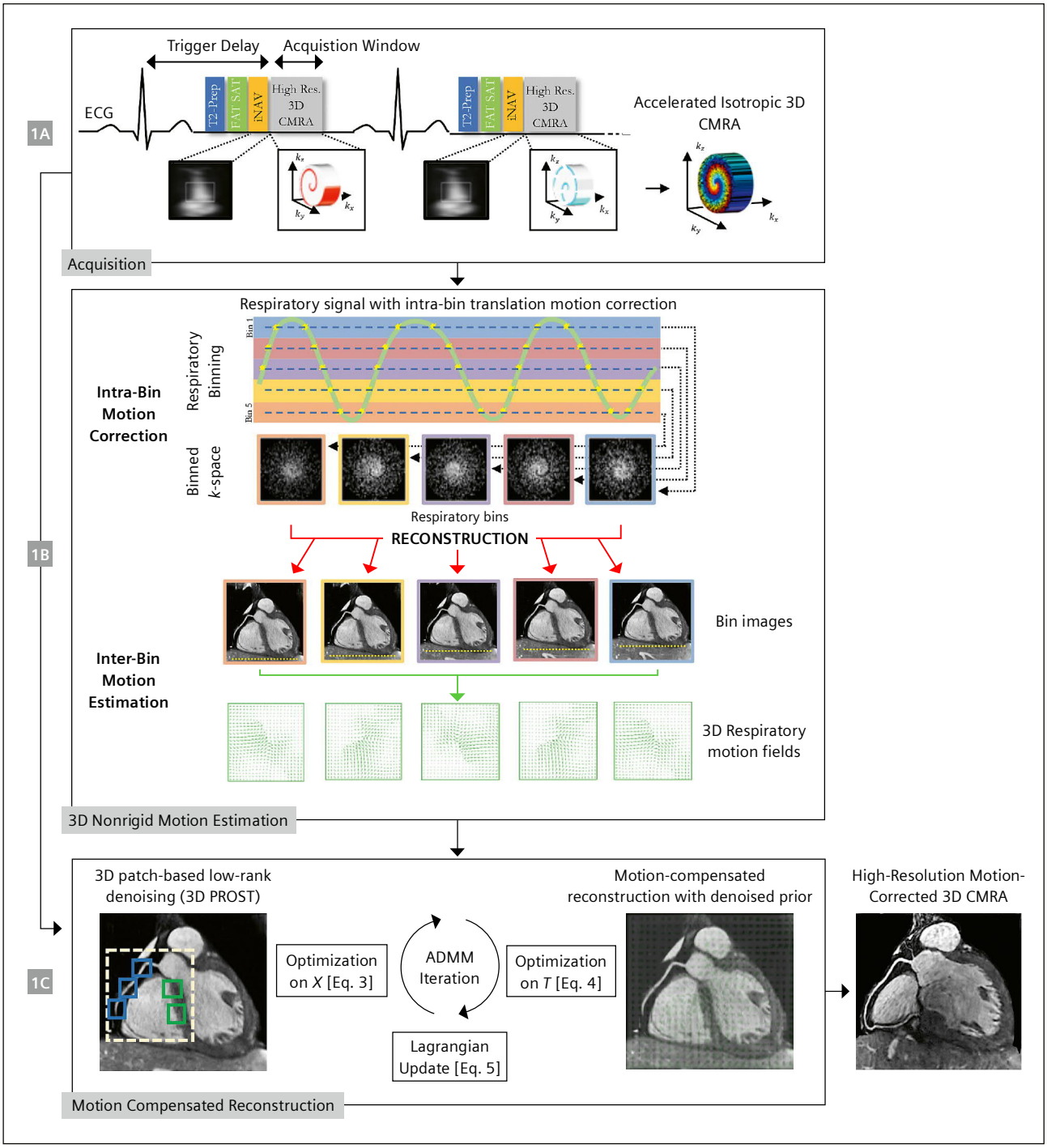

1 Schematic overview of the proposed accelerated free-breathing 3D CMRA acquisition with sub-millimeter isotropic resolution, 100% scan efficiency, and non-rigid motion-compensated PROST reconstruction. **(1A)** CMRA acquisition is performed with an undersampled 3D variable density spiral-like Cartesian trajectory with golden angle between spiral-like interleaves (VD-CASPR), preceded by 2D image navigators (iNAV) to allow for 100% scan efficiency, and beat-to-beat translational respiratory-induced motion correction of the heart. **(1B)** Foot-head respiratory signal is estimated from the 2D iNAVs and used to assign the acquired data to 5 respiratory bins and translation-corrected respiratory bins. Subsequent reconstruction of each bin is performed using soft-gated SENSE, and 3D non-rigid motion fields are then estimated from the 5 reconstructed datasets. **(1C)** The final 3D whole-heart motion-corrected CMRA image is obtained using the proposed 3D patch-based (PROST) non-rigid motion-compensated reconstruction.
Abbreviations: CMRA = coronary magnetic resonance angiography; PROST = patch-based undersampled reconstruction; ADMM = alternating direction method of multipliers.
Adapted and reproduced with permission from Bustin et al. [22].

agent. Large multi-center studies have demonstrated the clinical potential of coronary magnetic resonance angiography (CMRA) against X-ray coronary angiography for the anatomical assessment of CAD with per-patient sensitivity, specificity, and negative predictive value of up 94%, 82%, and 92% respectively [8–10]. However, widespread clinical implementation of CMRA is currently limited to suspected anomalous coronary arteries, suspected coronary artery aneurysms (e.g., Kawasaki's disease), coronary artery graft patency assessment, assessment of the proximal coronary arteries, and patients with renal impairment who are unable to receive iodinated contrast [11–13]. The very limited and specific clinical use of CMRA is due to long and unpredictable acquisition times, cumbersome scan planning, lower spatial resolution (usually 1–2 mm anisotropic), and motion-related (cardiac, respiratory, and patient) degradation of image quality.

In a similar fashion to CCTA, CMRA overcomes cardiac motion artifacts by using prospective electrocardiographic (ECG) gating to acquire data during the quiescent phase of the cardiac cycle when coronary artery motion is minimal [11], usually in mid-to-late diastole. In cases of cardiac arrhythmias and variable heart rates, which disproportionately impact the diastolic phase of the cardiac cycle, systolic imaging is the preferred option [11]. An alternative retrospective ECG gating approach is to continuously acquire data throughout the cardiac cycle and then reconstruct multiple cardiac phases and select the phase with the sharpest images or fewest motion artefacts [14, 15].

To compensate for the respiratory motion artifacts during free-breathing acquisitions, conventional CMRA estimates the respiratory displacement and deformation of the heart and surrounding tissues using the diaphragmatic 1D navigator approach [11, 16–18]. Here the liver-diaphragm interface lends itself for motion tracking, with the increased signal-to-noise ratio (SNR) of the right hemi diaphragm used as a surrogate to track the superior-inferior motion of the heart during the respiratory cycle, and with respiratory gating enabled to obtain image data at the quiescent phase of end of expiration [16, 19, 20, 17]. However, there is a non-linear relationship between the displacement of the diaphragm and the heart, requiring a patient-specific correction factor, which is usually set at 0.6 (population average) when gating is combined with respiratory motion correction [16]. Furthermore, only data within a small (end-expiration) respiratory gating window is accepted, significantly reducing scan efficiency and leading to prolonged and unpredictable acquisition times [21]. Moreover, prospective or retrospective translational motion compensation can only be applied in the superior-inferior direction [21]. Finally, this approach adds complexity as detailed scan planning and defining separate imaging parameters for the navigator acquisition are required, further increasing scan time and costs [16]. In addition, a fully sampled 3D whole-heart CMRA acquisition at high spatial resolution is associated with long acquisition times (up to 30 minutes), regardless of cardiac and respiratory motion gating, which leads to patient discomfort and patient-related motion artifacts.

To overcome these limitations, we have leveraged recent advances in CMR technology including trajectory design, motion correction, and undersampled reconstruction techniques – to propose a novel, highly accelerated, high-spatial-resolution (sub-1 mm^3), free-breathing, non-contrast, 3D whole-heart CMRA framework in a clinically feasible and 100% predictable acquisition time.

Proposed coronary magnetic resonance angiography framework

The proposed CMRA framework was developed on a 1.5T CMR scanner (MAGNETOM Aera, Siemens Healthcare, Erlangen, Germany) with a dedicated 32-channel spine coil and an 18-channel body coil. It combines a highly undersampled variable-density Cartesian acquisition with an image navigator (iNAV) to enable model-free 2D translational and 3D non-rigid motion estimation, and finally deploys a motion-corrected 3D patch-based low-rank image reconstruction (PROST) algorithm[1] to reconstruct the undersampled acquisition. These steps are outlined in more detail in the following sections and in the article by Bustin et al. [22].

Accelerated CMRA acquisition

An undersampled (3- to 4-fold) free-breathing 3D whole-heart, balanced steady-state free-precession (bSSFP) sequence with a 3D variable-density spiral-like Cartesian trajectory (VD-CASPR) with golden-angle step was employed as previously proposed [23] (Fig. 1). A low-resolution 2D iNAV preceded each spiral-like interleave to allow 100% scan efficiency, predictable scan time, and 2D translational motion estimation of the heart on a beat-to-beat basis. The 2D iNAVs were obtained by spatially encoding the startup profiles of the bSSFP sequence [24]. A spectrally selective SPIR (Spectral Presaturation with Inversion Recovery) fat saturation pulse with a constant flip angle (FA) of 130° was used to improve coronary depiction and minimize fat-related aliasing artifacts. An adiabatic T2 preparation pulse [25, 26] was played at each heartbeat in order to enhance the contrast between blood and cardiac muscle and to avoid the use of extracellular contrast agents.

[1] *Work in progress. The application is currently under development and is not for sale in the U.S. and in other countries. Its future availability cannot be ensured.*

Beat-to-beat 2D translational motion estimation
Beat-to-beat 2D translational motion correction was performed as previously proposed in [27, 28]. Briefly, foot-head (FH) and right-left (RL) translational respiratory motion of the heart was extracted from the iNAVs using a template-matching algorithm with normalized cross-correlation as similarity measure [24]. The reference template was manually selected during scan planning on a region encompassing the subject's heart. The FH respiratory signal was used to sort the acquired data into five respiratory states or bins. Intra-bin 2D translational motion estimation was performed by correcting the data for each bin to the same respiratory position (taken as the bin center) (Fig. 1). This correction was implemented by modulating the *k*-space data with a linear phase shift according to the previously estimated respiratory motion [27].

Bin-to-bin non-rigid motion estimation
In this framework, the acquired 3D CMRA data is undersampled (3- to 4-fold), with the resulting binned *k*-spaces being highly accelerated (~15- to 20-fold). Soft-gating iterative sensitivity encoding reconstruction [27] was employed to reconstruct each respiratory bin. Bin-to-bin 3D non-rigid motion estimation was subsequently performed using spline-based free-form deformation [29], considering the end-expiration bin as reference image (Fig. 1).

3D patch-based non-rigid motion-compensated reconstruction (non-rigid PROST)
Following this step, the estimated 3D non-rigid motion fields are then directly incorporated into a general matrix description reconstruction framework [30, 31]. In contrast to previous CMRA studies where the data are acquired either fully sampled [27] or with modest undersampling factors [28], our proposed high-resolution (0.9 mm^3) CMRA framework exploits higher undersampling factors (3- to 4-fold) to reach approximately 10-minute acquisition time. 3D patch-based low-rank undersampled reconstruction (3D PROST) has been proposed to highly accelerate sub-mm CMRA imaging with translational motion correction only [23]. 3D PROST reconstruction exploits the inherent redundancies of the complex 3D anatomy of the coronary arteries on a local (i.e., within a patch) and non-local (i.e., between similar patches within a neighborhood) basis, through an efficient iterative low-rank decomposition and singular value thresholding. The proposed non-rigid PROST framework combines 3D PROST with the matrix formalism for non-rigid motion correction, and can be formulated as the unconstrained optimization (found at the bottom of the page), where X is the non-rigid motion-corrected 3D CMRA volume (or "motion-free" image), K is the 2D translational motion-corrected k-space data, E is the encoding operator composed of: A_b the sampling matrix for bin b, F the 3D Fourier transform, S_c the coil sensitivities for coil c, U_b the estimated 3D non-rigid motion fields for bin b and N_{bins} the number of respiratory bins. $||.||_F$ and $||.||_*$ denote the Frobenius and nuclear norms respectively, $P_p(.)$ is the patch-selection operator at voxel p. Equation (1) can be efficiently solved by operator-splitting via alternating direction method of multipliers (ADMM).

Results from a single-center clinical study

The proposed CMRA framework was assessed in a cohort of patients with suspected CAD at Guy's and St Thomas' Hospitals, London, UK. The full results of this clinical study are described in the article by Hajhosseiny et al. [32]. In summary, 50 consecutive patients between 35 and 77 years of age who were referred for a clinically indicated CTCA were invited to undergo a CMRA within the proposed framework. In the absence of contraindications, each patient was treated with intravenous metoprolol in 5 mg increments with a maximum dose of 30 mg, aiming for a target heart rate (HR) < 65 bpm in order to maximize the diastolic acquisition window, reduce HR variability and cardiac motion artefacts. All patients were given 800 mg of sublingual glyceryl trinitrate to promote coronary vasodilation. To assess diagnostic performance, significant coronary stenosis was visually defined as luminal narrowing of ≥ 50% in each of the coronary segments using an intention-to-read approach. The image quality of CMRA images (3D whole-heart dataset and individual vessels) was evaluated using the following scale: 0, non-diagnostic; 1, poor (limited coronary vessel visibility or noisy image); 2, average (coronary vessel visible but diagnostic confidence low); 3, good (coronary artery adequately visualized and diagnostic quality image); and 4, excellent (coronary artery clearly depicted).

All CMRA acquisitions were successfully completed in an imaging time of 10.7 ± 1.4 min (range 8.0–13.3 min), with 100% respiratory scan efficiency. All CMRA acquisi-

(1) $$L_{NR\text{-}PROST}(X,T,Y) := \underset{X,T_p,Y}{\operatorname{argmin}} \| EX - K \|_F^2 + \lambda \sum_p \| T_p \|_* + \frac{\mu}{2} \sum_p \| T_p - P_p(X) - \frac{Y_p}{\mu} \|_F^2$$

(2) $$E = \sum_b^{N_{bins}} A_b F S_c U_b$$

tions were performed in diastole with an average acquisition window of 88 ± 8 ms (range 81–111 ms). Mean age was 55 ± 9 years, 33/50 (66%) were male, and 12/50 (24%) had significant CAD on CTCA.

In total, 95% of CMRA segments were deemed diagnostic, while all left main stem segments were diagnostic on CMRA. Furthermore, 97%, 96%, and 87% of right coronary artery, left anterior descending artery, and left circumflex artery segments were diagnostic on CMRA. Finally, 97%, 97%, and 90% of proximal, middle, and distal CMRA segments were of diagnostic quality.

The sensitivity, specificity, positive predictive value, negative predictive value, and diagnostic accuracy of CMRA for detecting significant CAD were as follows:

- per-patient
  100% (95% CI: 76–100%), 74% (95% CI: 58–85%), 55% (95% CI: 35–73%), 100% (95% CI: 88–100%), and 80% (95% CI: 67–89%) respectively;
- per-vessel
  81% (95% CI: 57–93%), 88% (95% CI: 82–93%), 46% (95% CI: 30–64%), 97% (95% CI: 93–99%), and 88% (95% CI: 81–92%) respectively;
- per-segment
  76% (95% CI: 55–89%), 95% (95% CI: 92–97%), 44% (95% CI: 30–60%), 99% (95% CI: 97–99%), and 94% (95% CI: 91–96%) respectively.

Example images from selected patients with suspected CAD are shown in Figures 2–8.

The proposed CMRA framework (without PROST regularization) has been implemented in-line in the scanner software, providing non-rigid motion corrected reconstructions in ~2–5 min (CPU).

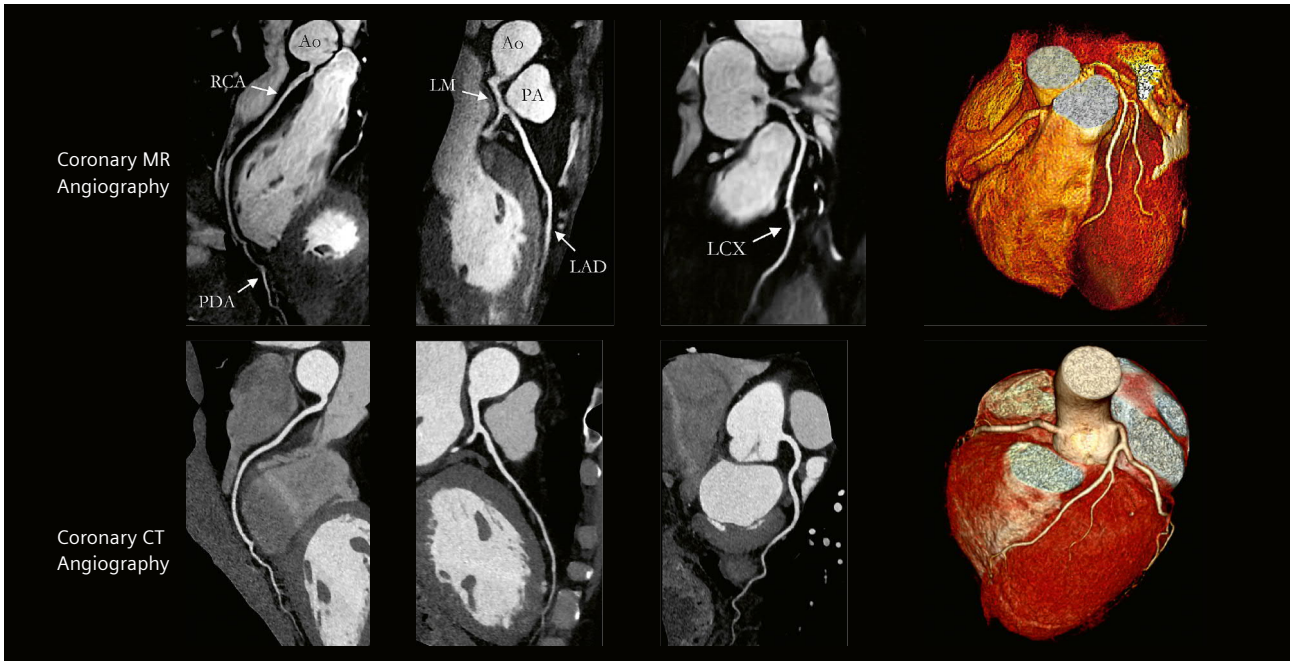

2 Non-contrast whole-heart sub-millimeter isotropic CMRA images of a 53-year-old male patient with normal coronary arteries. Accelerated free-breathing CMRA images acquired and reconstructed with the proposed framework are shown in the top row, revealing the LAD, RCA, and LCX territories. The corresponding reformatted images obtained with contrast-enhanced CCTA are shown in the bottom row. 3D volume-rendered images for both modalities are shown in the right-hand column.
Abbreviations: CMRA = coronary magnetic resonance angiography; CCTA = coronary computed tomography angiography; LAD = left anterior descending artery; RCA = right coronary artery; LCX =left circumflex artery; PDA = posterior descending artery; PA = pulmonary artery; Ao = aorta.
Adapted and reproduced with permission from Bustin et al. [22].

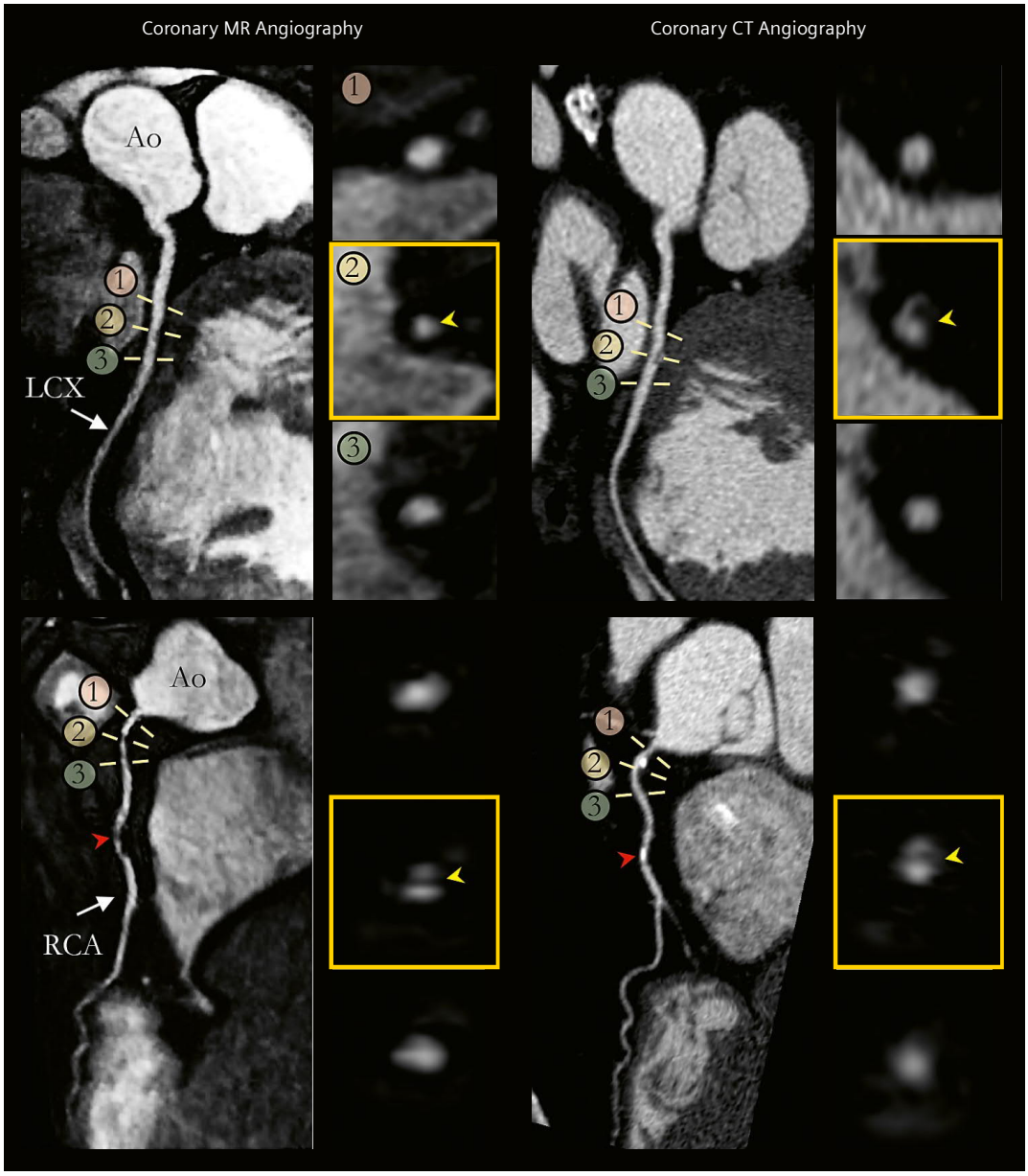

3 Reformatted non-contrast whole-heart sub-millimeter isotropic CMRA (left) and contrast-enhanced CCTA (right) images along the LCX (top) and RCA (bottom) are shown for a 54-year-old male patient. The CCTA images demonstrate mild (< 50%) disease with a calcified plaque within the proximal RCA, severe disease (> 50%) with a partially calcified plaque in the mid-segment of the RCA (red arrows), and mild (< 50%) disease with calcified plaque in the mid-segment of the LCX. Luminal narrowing is seen on the cross-sectional views at the sites of coronary plaque on the CMRA images (yellow arrows).
Abbreviations: CMRA = coronary magnetic resonance angiography; CCTA = coronary computed tomography angiography; LAD = left anterior descending artery; RCA = right coronary artery; LCX = left circumflex artery; Ao = aorta.
Adapted and reproduced with permission from Bustin et al. [22].

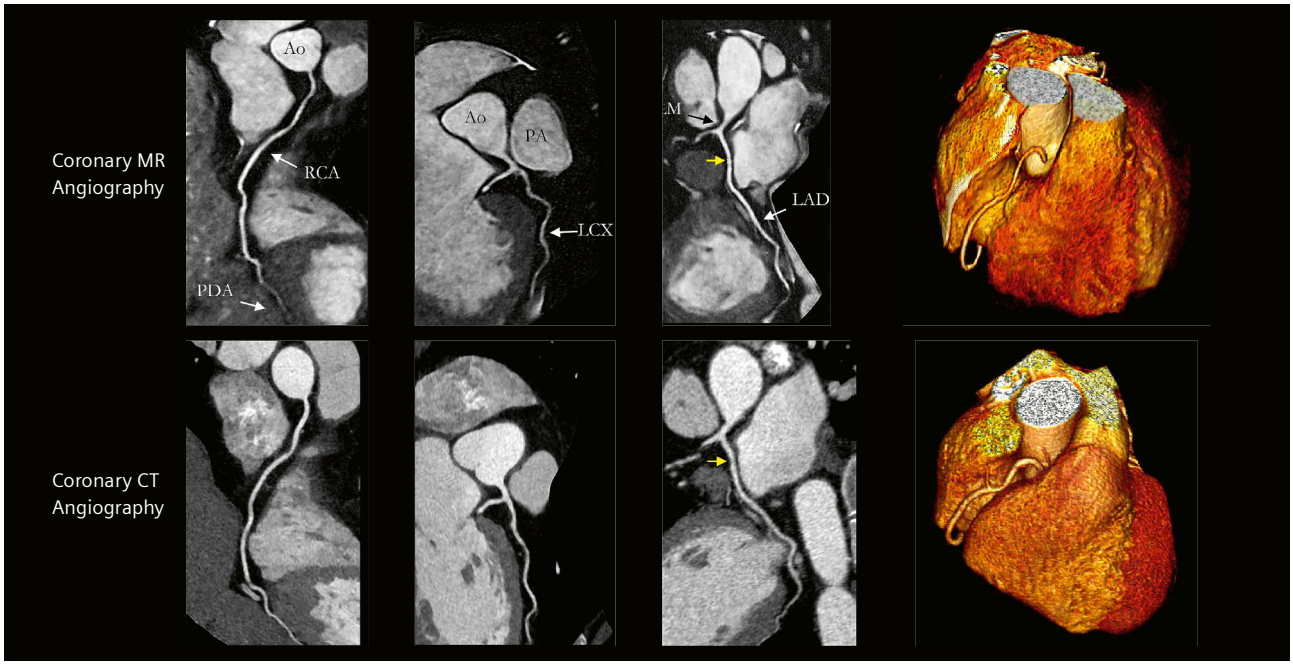

4 Non-contrast whole-heart sub-millimeter isotropic CMRA images of a 35-year-old male patient with normal coronary arteries. The CMRA images acquired and reconstructed with the proposed framework are shown in the top row, revealing the LAD and RCA. The corresponding reformatted images obtained with contrast-enhanced CCTA are shown in the bottom row. The 3D volume-rendered images are shown in the right-hand column, which were both correctly visualized on the CMRA images.
Abbreviations: CMRA = coronary magnetic resonance angiography; CCTA = coronary computed tomography angiography; LAD = left anterior descending artery; RCA = right coronary artery; LCX = left circumflex artery; LM = left main stem; PDA = posterior descending artery; PA = pulmonary artery; Ao = aorta.
Adapted and reproduced with permission from Bustin et al. [22].

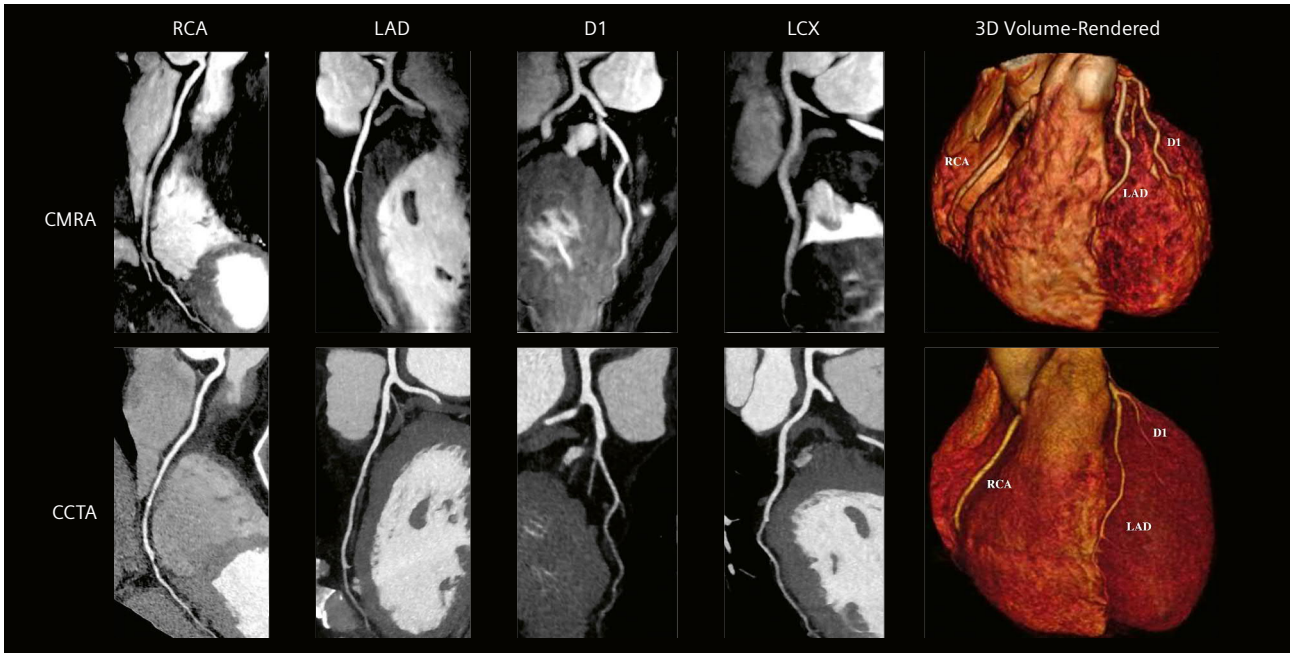

5 Curved multiplanar reformat and 3D volume-rendered non-contrast CMRA and contrast-enhanced CCTA in a 54-year-old male with no significant stenosis.
Abbreviations: CMRA = coronary magnetic resonance angiography; CCTA = coronary computed tomography angiography; RCA = right coronary artery; LAD = left anterior descending artery; D1 = first diagonal artery; LCX = left circumflex artery.
Adapted and reproduced with permission from Hajhosseiny et al. [32].

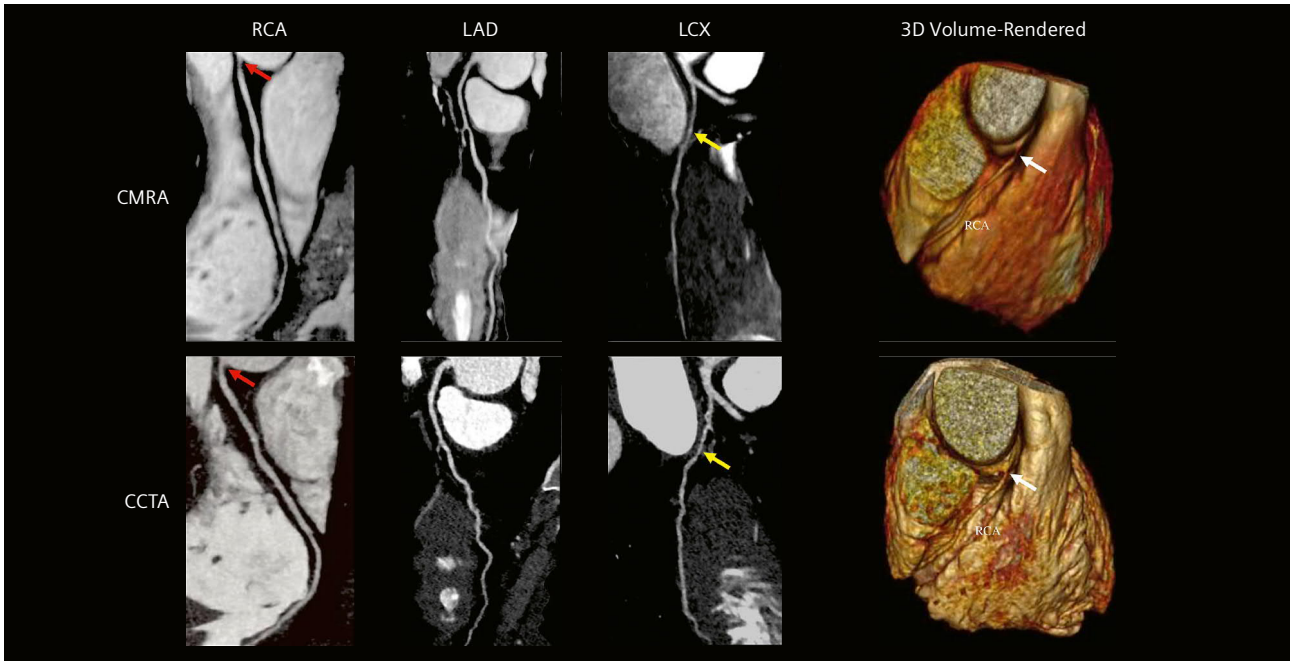

6 Curved multiplanar reformat and 3D volume-rendered non-contrast CMRA and contrast-enhanced CCTA in a 44-year-old male with > 50% non-calcified stenosis in the ostial RCA (red arrows). This can also be seen in the 3D volume-rendered images (white arrows). The yellow arrows represent a > 50% stenosis in the proximal/mid LCX.
Abbreviations: CMRA = coronary magnetic resonance angiography; CCTA = coronary computed tomography angiography; RCA = right coronary artery; LAD = left anterior descending artery; LCX = left circumflex artery.
Adapted and reproduced with permission from Hajhosseiny et al. [32].

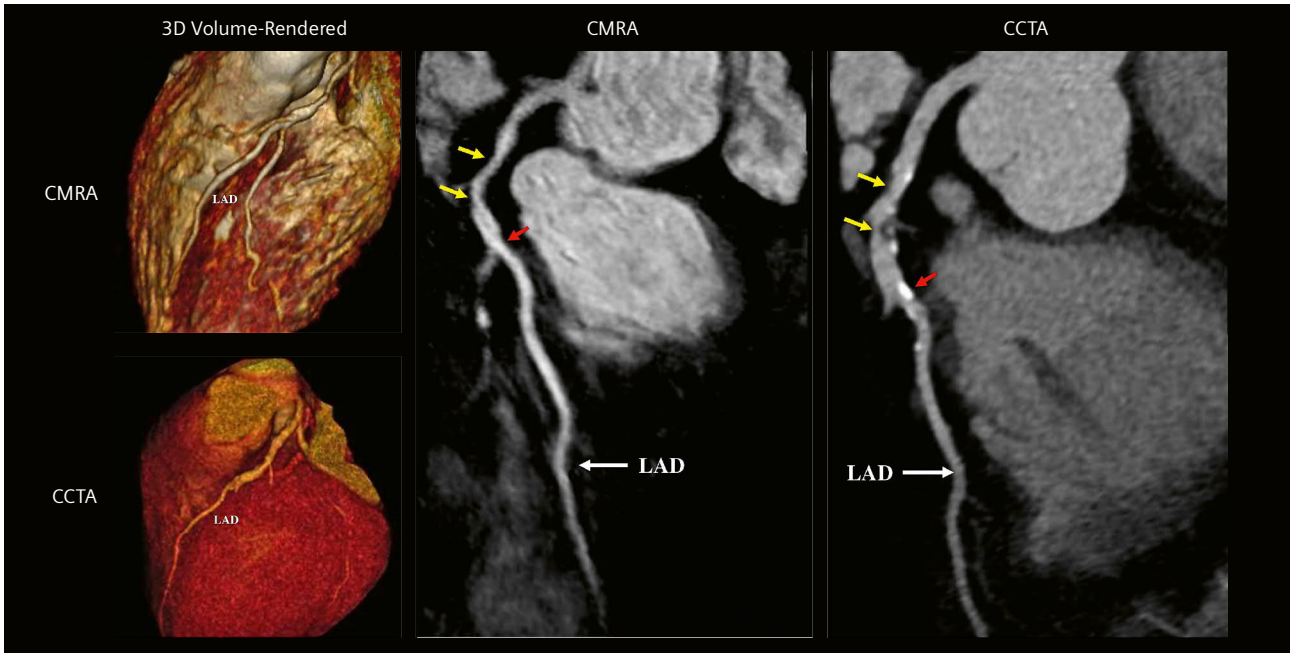

7 Curved multiplanar reformat and 3D volume-rendered non-contrast CMRA and contrast-enhanced CCTA in a 60-year-old male with > 50% partially calcified stenosis in the proximal-to-mid LAD on either side of the first diagonal artery (yellow arrows). The red arrows point to a focal calcified < 50% stenosis just distal to the second diagonal artery.
Abbreviations: CMRA = coronary magnetic resonance angiography; CCTA = coronary computed tomography angiography; LAD = left anterior descending artery. *Adapted and reproduced with permission from Hajhosseiny et al. [32].*

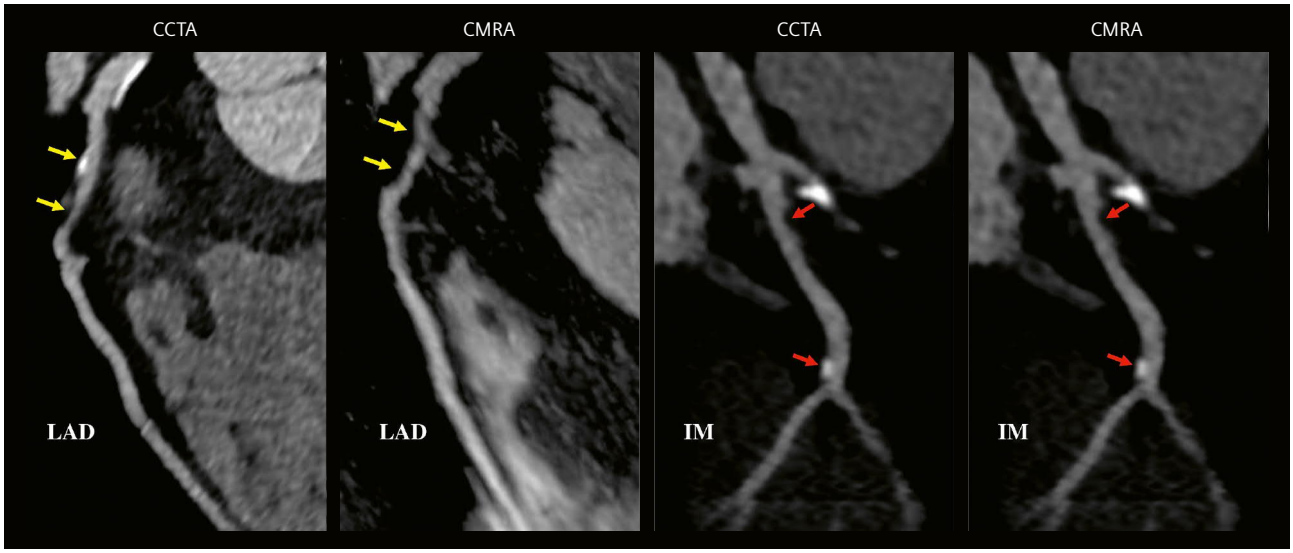

8 Curved multiplanar reformat non-contrast CMRA and contrast-enhanced CCTA in a 57-year-old male with > 50% partially calcified stenosis in the proximal LAD (yellow arrows). The red arrows point to focal < 50% stenosis in the proximal and distal ramus intermedius artery. **Abbreviations:** CMRA = coronary magnetic resonance angiography; CCTA = coronary computed tomography angiography; LAD = left anterior descending artery; IM = ramus intermedius artery. *Adapted and reproduced with permission from Hajhosseiny et al. [32].*

Conclusions

In this initial single-center clinical study, we have introduced a robust, contrast-free, sub-millimeter CMRA framework with predictable and clinically feasible scan times of approximately 10 minutes, achieving highly diagnostic image quality and diagnostic accuracy for excluding significant disease in patients with suspected CAD. This is the first clinical study to assess the diagnostic performance of a 3D contrast-free CMRA approach that enables a predictable scan time of approximately 10 minutes for 0.9 mm^3 spatial-resolution. This was achieved by employing a robust motion corrected free-breathing acquisition with 100% respiratory scan efficiency, using image navigation for 2D translational motion estimation and respiratory data binning combined with 3D non-rigid motion compensated undersampled reconstruction employing a 3- to 4-fold undersampled Cartesian acquisition and a patched-based low-rank reconstruction. Future work will focus on multi-center clinical assessment of this novel framework to determine its clinical applicability in a larger cohort of patients with a wider spectrum of CAD.

References

1 Benjamin EJ, Virani SS, Callaway CW, et al. Heart disease and stroke statistics-2018 update: A report from the American Heart Association. Circulation 2018;137(12):e67–e492. Available at: http://www.ncbi.nlm.nih.gov/pubmed/29386200.

2 Kočka V. The coronary angiography – An old-timer in great shape. Cor Vasa 2015;57(6):e419–e424. Available at: https://www.sciencedirect.com/science/article/pii/S0010865015001009. Accessed August 14, 2018.

3 Tavakol M, Ashraf S, Brener SJ. Risks and complications of coronary angiography: a comprehensive review. Glob J Health Sci. 2012;4(1):65–93. Available at: http://www.ncbi.nlm.nih.gov/pubmed/22980117. Accessed August 14, 2018.

4 Kolossváry M, Szilveszter B, Merkely B, Maurovich-Horvat P. Plaque imaging with CT-a comprehensive review on coronary CT angiography based risk assessment. Cardiovasc Diagn Ther. 2017;7(5):489–506. Available at: http://www.ncbi.nlm.nih.gov/pubmed/29255692. Accessed August 14, 2018.

5 Hamilton M, Baumbach A. Non invasive coronary imaging with computed tomography. [journal on the Internet]. 2007; 5(20). Available at: https://www.escardio.org/Journals/E-Journal-of-Cardiology-Practice/Volume-5/Non-Invasive-Coronary-Imaging-With-Computed-Tomography-Title-Non-Invasive-Cor. Accessed August 14, 2018.

6 Alfakih K, Byrne J, Monaghan M. CT coronary angiography: a paradigm shift for functional imaging tests. Open Hear. 2018;5(1):e000754. Available at: http://www.ncbi.nlm.nih.gov/pubmed/29632679. Accessed August 14, 2018.

7 Doris MK, Newby DE. How should CT coronary angiography be integrated into the management of patients with chest pain and how does this affect outcomes? Eur Heart J - Qual Care Clin. Outcomes 2016;2(2):72–80. Available at: https://academic.oup.com/ehjqcco/article-lookup/doi/10.1093/ehjqcco/qcv027. Accessed August 14, 2018.

8 Kim WY, Danias PG, Stuber M, et al. Coronary magnetic resonance angiography for the detection of coronary stenoses. N Engl J Med. 2001;345(26):1863–1869. Available at: http://www.ncbi.nlm.nih.gov/pubmed/11756576. Accessed July 26, 2019.

9 Yang Q, Li K, Liu X, et al. Contrast-Enhanced Whole-Heart Coronary Magnetic Resonance Angiography at 3.0-T. A Comparative Study With X-ray Angiography in a Single Center. J Am Coll Cardiol. 2009;54(1):69-76.

10 Kato S, Kitagawa K, Ishida N, et al. Assessment of coronary artery disease using magnetic resonance coronary angiography: a national multicenter trial. J Am Coll Cardiol. 2010;56(12):983–91. Available at: http://linkinghub.elsevier.com/retrieve/pii/S0735109710024691. Accessed September 30, 2018.
11 Sriharan M, McParland P, Harden S, Nicol E. Non-Invasive Coronary Angiography. In: Branislav B. Coronary Angiography - Advances in Noninvasive Imaging Approach for Evaluation of Coronary Artery Disease. [book on the Internet]. London: InTech, 2011:99-122. DOI: 10.5772/22475. Available at: http://www.intechopen.com/books/coronary-angiography-advances-in-noninvasive-imaging-approach-for-evaluation-of-coronary-artery-disease/non-invasive-coronary-angiography. Accessed August 16, 2018.
12 Mangla A, Oliveros E, Williams KA, Kalra DK. Cardiac imaging in the diagnosis of coronary artery disease. Curr Probl Cardiol. 2017;42(10):316–366. Available at: https://www.sciencedirect.com/science/article/pii/S0146280617300725?via%3Dihub#bib116. Accessed August 16, 2018.
13 Hamdy A, Ishida M, Sakuma H. Cardiac MR assessment of coronary arteries. CVIA 2017;1(1):49–59. Available at: https://doi.org/10.22468/cvia.2016.00066. Accessed December 11, 2018.
14 Coppo S, Piccini D, Bonanno G, et al. Free-running 4D whole-heart self-navigated golden angle MRI: Initial results. Magn Reson Med. 2015;74(5):1306–1316. Available at: http://www.ncbi.nlm.nih.gov/pubmed/25376772. Accessed September 3, 2018.
15 Pang J, Bhat H, Sharif B, et al. Whole-heart coronary MRA with 100% respiratory gating efficiency: Self-navigated three-dimensional retrospective image-based motion correction (TRIM). Magn Reson Med. 2014;71(1):67–74. Available at: http://doi.wiley.com/10.1002/mrm.24628. Accessed August 18, 2018.
16 Henningsson M, Botnar RM. Advanced respiratory motion compensation for coronary MR angiography. Sensors (Basel). 2013;13(6):6882–99. Available at: http://www.ncbi.nlm.nih.gov/pubmed/23708271. Accessed August 17, 2018.
17 Ehman RL, Felmlee JP. Adaptive technique for high-definition MR imaging of moving structures. Radiology 1989;173(1):255–263. Available at: http://www.ncbi.nlm.nih.gov/pubmed/2781017. Accessed August 17, 2018.
18 McConnell M V, Khasgiwala VC, Savord BJ, et al. Comparison of respiratory suppression methods and navigator locations for MR coronary angiography. AJR Am J Roentgenol. 1997;168(5):1369–1375. Available at: http://www.ncbi.nlm.nih.gov/pubmed/9129447. Accessed August 17, 2018.
19 Danias PG, McConnell M V, Khasgiwala VC, Chuang ML, Edelman RR, Manning WJ. Prospective navigator correction of image position for coronary MR angiography. Radiology. 1997;203(3):733–736. Available at: http://www.ncbi.nlm.nih.gov/pubmed/9169696. Accessed August 17, 2018.
20 Nehrke K, Börnert P, Groen J, Smink J, Böck JC. On the performance and accuracy of 2D navigator pulses. Magn Reson Imaging 1999;17(8):1173–81. Available at: http://www.ncbi.nlm.nih.gov/pubmed/10499679. Accessed August 17, 2018.
21 Correia T, Ginami G, Cruz G, et al. Optimized respiratory-resolved motion-compensated 3D Cartesian coronary MR angiography. Magn Reson Med. 2018;80(6):2618–2629. Available at: http://www.ncbi.nlm.nih.gov/pubmed/29682783. Accessed August 17, 2018.
22 Bustin A, Rashid I, Cruz G, et al. 3D whole-heart isotropic sub-millimeter resolution coronary magnetic resonance angiography with non-rigid motion-compensated PROST. J Cardiovasc Magn Reson. 2020;22(1):https://doi.org/10.1186/s12968-020-00611-5.
23 Bustin A, Ginami G, Cruz G, et al. Five-minute whole-heart coronary MRA with sub-millimeter isotropic resolution, 100% respiratory scan efficiency, and 3D-PROST reconstruction. Magn Reson Med. 2019;81(1):102–115.
24 Henningsson M, Koken P, Stehning C, Razavi R, Prieto C, Botnar RM. Whole-heart coronary MR angiography with 2D self-navigated image reconstruction. Magn Reson Med. 2012;67(2):437–445. Available at: http://www.ncbi.nlm.nih.gov/pubmed/21656563. Accessed August 17, 2018.
25 Nezafat R, Stuber M, Ouwerkerk R, Gharib AM, Desai MY, Pettigrew RI. B1-insensitive T2 preparation for improved coronary magnetic resonance angiography at 3T. Magn Reson Med. 2006;55(4):858–64.
26 Botnar RM, Stuber M, Danias PG, Kissinger K V, Manning WJ. Improved coronary artery definition with T2-weighted, free-breathing, three-dimensional coronary MRA. Circulation. 1999;99(24):3139–3148.
27 Cruz G, Atkinson D, Henningsson M, Botnar RM, Prieto C. Highly efficient nonrigid motion-corrected 3D whole-heart coronary vessel wall imaging. Magn Reson Med. 2017;77(5):1894–1908. Available at: http://doi.wiley.com/10.1002/mrm.26274. Accessed August 20, 2018.
28 Correia T, Cruz G, Schneider T, Botnar RM, Prieto C. Technical note: Accelerated nonrigid motion-compensated isotropic 3D coronary MR angiography. Med Phys. 2018;45(1):214–222.
29 Rueckert D, Sonoda LI, Hayes C, Hill DL, Leach MO, Hawkes DJ. Nonrigid registration using free-form deformations: application to breast MR images. IEEE Trans Med Imaging. 1999;18(8):712–721.
30 Batchelor PG, Atkinson D, Irarrazaval P, Hill DLG, Hajnal J, Larkman D. Matrix description of general motion correction applied to multishot images. Magn Reson Med. 2005;54(5):1273–1280.
31 Cruz G, Atkinson D, Buerger C, Schaeffter T, Prieto C. Accelerated motion corrected three-dimensional abdominal MRI using total variation regularized SENSE reconstruction. Magn Reson Med. 2016;75(4):1484–1498.
32 Hajhosseiny R, Rashid I, Bustin A, Munoz C, Cruz G, Nazir M.S, Grigoryan K, Ismail T.F, Preston R, Neji R, Kunze K, Razavi R, Chiribiri A, Masci P.G, Rajani R, Prieto C, Botnar R.M. Clinical comparison of sub-mm high-resolution non-contrast coronary MRA against coronary CTA in patients with low-intermediate risk of CAD: A single center trial. J Cardiovasc Magn Reson. 2021; IN PRESS.

Contact

Reza Hajhosseiny, M.D.
School of Biomedical Engineering and Imaging Sciences
King's College London
3rd floor Lambeth Wing
London, SE1 7EH
United Kingdom
Phone: +44 020 7188 7188
reza.hajhosseiny@kcl.ac.uk
Twitter: @KCL_CardiacMR